Research Article

Assessment of the Use of Epicarp and Mesocarp of Green Coconut for Removal of Fluoride Ions in Aqueous Solution

César Augusto Canciam [iD][1] **and Nehemias Curvelo Pereira**[2]

[1]*M.Sc. in Chemical Engineering, Academic Department of Chemical Engineering, Federal University of Technology-Paraná, Ponta Grossa, Brazil*
[2]*Ph.D. in Chemical Engineering, Chemical Engineering Department, State University of Maringá, Maringá, Brazil*

Correspondence should be addressed to César Augusto Canciam; canciam@utfpr.edu.br

Fruit consumption and processing result in considerable volumes of residual biomass. Transformation of this biomass into biosorbents offers an alternative for its reuse and disposal. As the green coconut shell is a waste often discarded in landfills and dumps, generating gases and leachate, two biosorbents were developed from the epicarp and mesocarp of green coconut to adsorb fluoride ions in aqueous solution. The kinetic experiments showed that sorption of fluoride ions reached equilibrium at 300 min for both epicarp and mesocarp at temperatures of 25°C, 35°C, and 45°C. The removal efficiency of fluoride ions varied from 66.25% (at 25°C) to 77.50% (at 45°C) for the epicarp and from 90% (at 25°C) to 97.50% (at 45°C) for the mesocarp. The thermodynamic parameters of the adsorption process showed that adsorption is a spontaneous, endothermic process for both biosorbents. The adsorption was classified as chemical, with the Langmuir isotherm model best suited to the adsorption isotherms data.

1. Introduction

Groundwater from countries such as Algeria, Argentina, Australia, Bangladesh, China, South Korea, Egypt, Spain, United States, Ghana, India, Iran, Iraq, Israel, Italy, Japan, Jordan, Libya, Mexico, Morocco, New Zealand, Kenya, Senegal, South Africa, Sri Lanka, Tanzania, and Turkey, as well as countries in South America, is contaminated with fluoride ions. The concentration of fluoride ions can vary from 0.5 to $50\,mg{\cdot}L^{-1}$, depending on geological factors [1–6].

Although the maximum acceptable concentration of fluoride ions in drinking water established by the World Health Organization is $1.5\,mg{\cdot}L^{-1}$, some countries have adopted other limits. For example, South Africa's acceptable limit is $0.75\,mg{\cdot}L^{-1}$ [7].

In small concentrations, fluoride ions help to prevent dental caries and improve calcification of dental enamel. At high concentrations, however, they can interfere with the functioning of the kidneys, thyroid, parathyroid, liver, testes, and neurons [7–10].

In adults, concentrations of fluoride ions greater than $1.5\,mg{\cdot}L^{-1}$ can lead to dental fluorosis, while concentrations above $3\,mg{\cdot}L^{-1}$ can cause skeletal fluorosis. It is estimated that 26 million people in China suffer from dental fluorosis and 1 million from skeletal fluorosis, due to the consumption of water contaminated with high levels of fluoride ions [11–14].

Dental fluorosis is a major public health problem because in moderate or severe forms, it causes functional and aesthetic alterations that interfere with personality formation and integration into the labour market, requiring highly complex dental treatment. In general, the clinical aspect of dental fluorosis ranges from opaque spots on the enamel to yellowish or brown areas in the case of more severe changes [15].

Skeletal fluorosis is a serious condition, resulting from chronic ingestion of large amounts of fluoride over many years during periods of bone modelling (growth) and/or remodelling. Skeletal fluorosis manifests as an increase in bone density leading to thickening of the long bones and calcification of the ligaments. Symptoms include mild rheumatic pains, arthritis of the joints and muscles, and pain along the cervical spine.

Skeletal fluorosis causes bending of the legs outwards from the knees, and in more advanced cases, the person is unable to move around and remains bedridden [9, 13].

The various processes for the removal of fluoride ions from water include coagulation and chemical precipitation, membrane processes (dialysis, nanofiltration, and reverse osmosis), electrolytic treatment (electrodialysis and electrocoagulation), and ion exchange and adsorption. The adsorption process used in the removal of fluoride ions offers greater accessibility, low cost, and simple design and operation. Disadvantages are that this process requires pH adjustment, while the presence of other dissolved ions may interfere with the adsorption of fluoride ions [7, 16].

Although the green coconut shell is a residue of coconut water use and industrialisation with great potential for reuse, few attempts have been made to exploit it, with most shells deposited in dumps and landfills, causing an environmental problem. The green coconut shell is not easily degradable (taking about 8 years), occupies a lot of space in the landfills, and causes the proliferation of diseases [17, 18].

Coconut fruit (*Cocos nucifera* L.) consists of epicarp, mesocarp, endocarp, embryo, copra, and coconut water. The epicarp is the outer layer with a smooth surface, coated with wax. The mesocarp is the middle layer, the more developed and voluminous part of the fruit. Epicarp, mesocarp, and endocarp make up 80–85% of the mass of the immature fruit [17, 19].

As a biosorbent, the green coconut shell has been studied mainly in the removal of cations, with few studies devoted to the removal of anions using this type of biosorbent [20]. The objective of this study was thus to characterise the biosorbents (the analysis of the textural properties and the identification of the functional groups that participate in the adsorption process by means of Fourier transform infrared spectroscopy) and investigate the kinetics, equilibrium, and thermodynamics in the adsorption of fluoride ions using the epicarp and mesocarp of green coconut in a batch process.

2. Materials and Methods

2.1. Materials. The green coconut samples used in this study came from the disposal of material after the consumption of coconut water and were provided by a company located in Maringá, Paraná, Brazil.

The green coconut was peeled manually with a special knife, giving slices of epicarp approximately 3 mm thick and mesocarp approximately 5 mm thick, which were then dried separately at 70°C in a convective upflow air drier. The drying times at equilibrium were determined at 141 min and 140 min, respectively, for the epicarp and the mesocarp. After drying, the materials were crushed separately and sorted by size, using laboratory sieves. The fractions of adsorbents used in the study had an average diameter of 0.75 mm.

2.2. Characterisation of the Biosorbents. In order to characterise the biosorbents, analysis of the textural properties (specific surface area, specific volume, and average radius of the pores) and identification of the functional groups that participate in the adsorption process by means of the Fourier transform infrared spectroscopy (FTIR) were carried out.

Analysis of textural properties was carried out using NOVA 1000 series Quantachrome and data analysis with NovaWin version 10.01. The method used was nitrogen adsorption and desorption method at 77 K, using dry epicarp and mesocarp at 70°C, with particles with a mean diameter of 0.75 mm.

The functional groups that participate in the adsorption process were determined by means of the infrared spectrophotometer with Fourier transform (Frontier-PerkinElmer), in the infrared range between 400 and 4,000 cm^{-1}. In the FTIR, the spectra of the samples before and after adsorption of the fluoride ions were determined.

2.3. Adsorption Kinetics. The experiments were carried out in batch, using a cooled incubator with shaking (Tecnal, model TE-421). In the experiments, 0.50 g of each biosorbent was used in a series of flasks containing 30 mL of an aqueous solution of sodium fluoride, with an initial concentration of fluoride ions 4 mg·L^{-1}. The flasks were shaken mechanically at 150 rpm, at predetermined times (5, 10, 15, 20, 30, 45, 60, 120, 180, 210, 240, 270, 300, 330, 360, 390, and 420 minutes) and maintained at 25, 35, and 45°C. The pH of the solution was 8.0.

The SPADNS colorimetric method was employed for the determination of the concentration of fluoride ions [21].

The percentage of fluoride ions removed from the aqueous solution was calculated by the following equation:

$$R(\%) = \frac{C_0 - C_e}{C_0} \cdot 100, \tag{1}$$

where C_0 and C_e represent initial and equilibrium concentrations (mg·L^{-1}), respectively, and $R(\%)$ is the fluoride ion removal efficiency (%).

The adsorption capacity as a function of time can be expressed as follows [22]:

$$q(t) = \frac{[C_0 - C(t)] \cdot V}{m}, \tag{2}$$

where $q(t)$ is the adsorption capacity as a function of time (mg·g^{-1}), V is the volume of the treated solution (L), m is the mass of adsorbent (g), and $C(t)$ is the final time fluoride concentration in the solution (mg·L^{-1}).

The experimental adsorption kinetic data were modelled by pseudo-first-order and pseudo-second-order kinetics models, the Elovich model, and the intraparticle diffusion model, which are represented in their nonlinear forms by the following equations [23–25].

Pseudo-first-order model:

$$q(t) = q_e \cdot \left[1 - e^{(-k_1 \cdot t)}\right]. \tag{3}$$

Pseudo-second-order model:

$$q(t) = \frac{k_2 \cdot q_e^2 \cdot t}{1 + (q_e \cdot k_2 \cdot t)}. \tag{4}$$

Elovich model:

$$q(t) = \frac{1}{\beta} \cdot \ln(\alpha \cdot \beta \cdot t). \tag{5}$$

Intraparticle diffusion model:

$$q(t) = \left(k_{\text{dif}} \cdot \sqrt{t}\ \right) + C_{\text{d}}, \qquad (6)$$

where q_{e} is the quantity of fluoride ions adsorbed at equilibrium by mass of biosorbents (mg·g^{-1}); t is the time (min); k_1 and k_2 are, respectively, the pseudo-first-order rate constant (min^{-1}) and pseudo-second-order rate constant (g·mg^{-1}·min^{-1}); α is the initial adsorption velocity in the Elovich model (mg·g^{-1}·min^{-1}); β is a parameter of the Elovich model (g·mg^{-1}); k_{dif} is the intraparticle diffusion rate constant (mg·g^{-1}·min$^{-0.5}$); and C_{d} is the constant in the intraparticle diffusion model (mg·g^{-1}).

2.4. Adsorption Isotherms.
In the in-batch experiments, 0.50 g of each biosorbent was used in a series of flasks containing 30 mL of aqueous solutions of sodium fluoride, with initial concentrations of fluoride ions of 4, 5, 8, 10, 12, and 14 mg·L^{-1}. The flasks were shaken mechanically at 150 rpm for 24 hours and maintained at 25, 35, and 45°C. The pH of the solutions was 8.0.

The Langmuir and Freundlich isotherm models were suited to the experimental data. Nonlinear regression analysis was performed using OringinPro8 software.

The nonlinear forms of the Langmuir and Freundlich isotherm models can be expressed as follows [26, 27].

Langmuir isotherm model:

$$q_{\text{e}} = \frac{q_{\text{max}} \cdot k_{\text{L}} \cdot C_{\text{e}}}{1 + \left(k_{\text{L}} \cdot C_{\text{e}}\right)}. \qquad (7)$$

Freundlich isotherm model:

$$q_{\text{e}} = k_{\text{F}} \cdot C_{\text{e}}^{(1/n)}, \qquad (8)$$

where q_{e} is the concentration of fluoride ions after reaching equilibrium (mg·L^{-1}); C_{e} is quantity of fluoride ions retained in the adsorbent at equilibrium by mass of adsorbent (mg·g^{-1}); q_{max} is the maximum adsorption capacity (mg·g^{-1}); k_{L} and k_{F} are, respectively, the Langmuir constant (L·mg^{-1}) and the Freundlich constant (mg$^{(n-1/n)}$·L$^{1/n}$); and n is Freundlich's exponent (dimensionless).

2.5. Selection of Models.
All experiments were carried out in duplicates, and the reported values were averages.

In the selection of models, Akaike's criterion for small samples (AIC$_{\text{c}}$) was applied. The best-fit model for the experimental data corresponds to the model that had the smallest value of Akaike's criterion for small samples [28]. This criterion is given by the following equation:

$$\text{AIC}_{\text{c}} = \left[n_{\text{e}} \cdot \ln\left(\frac{\text{SQE}}{n_{\text{e}}}\right)\right] + \left(2 \cdot n_{\text{p}}\right) + \left[\frac{\left(2 \cdot n_{\text{p}}\right) \cdot \left(n_{\text{p}} + 1\right)}{n_{\text{e}} - n_{\text{p}} - 1}\right], \qquad (9)$$

where SQE is the sum of squares of errors and n_{e} and n_{p} are the number of experimental observations and of model parameters, respectively.

3. Results and Discussion

3.1. Characterisation of the Biosorbents.
Table 1 lists the specific surface area, the specific volume of mesopores, the specific volume of micropores, the mean radius of the mesopores, and the mean radius of the micropores of the dried epicarp and mesocarp of green coconut at 70°C.

The drying causes damage to the cellular structure of the materials, leading to a change in shape and decrease in size [29]. Crushing leads to a decrease in particle size and an increase in the specific surface area [30]. Thus, before adsorption, the biosorbents were damaged by the drying process and showed an increased specific surface area due to crushing. In Table 1, it can be seen that the mesocarp had a greater specific surface area in relation to the epicarp.

The infrared vibrational spectra of the epicarp of green coconut (before and after the adsorption of fluoride ions) are shown in Figure 1, which shows absorption bands of 1,059, 1,520, 1,615, and 2,921 cm^{-1}.

The absorption band at 1,059 cm^{-1} was attributed to the stretching of the high-intensity C-O group, which can be found in alcohols, ethers, esters, carboxylic acids, and anhydrides. The absorption band at 1,520 cm^{-1} was attributed to the C-H group, which can be found in alkenes and is a characteristic of off-plan folding. The absorption band at 1,615 cm^{-1} was attributed to the stretching of the C=C group, while the absorption band at 2,921 cm^{-1} was attributed to the stretching of the high-intensity C-H group, found in alkanes [31].

The infrared vibrational spectra of the mesocarp of green coconut (before and after the adsorption of fluoride ions) are shown in Figure 2.

The absorption bands at 1,520 cm^{-1} and 1,615 cm^{-1} were attributed to off-plane folding of the C-H group and to the stretching of the C=C group, respectively. The absorption band in 2,930 cm^{-1} was attributed to the stretching of the high-intensity C-H group, while the absorption band at 3,353 cm^{-1} was attributed to the C=C group of the aromatic ring [31].

The C=C group is found in lignin and chlorophyll. The C-O group is found in cellulose, hemicelluloses, pectin, lignin, tannins, and chlorophyll. The C-H group is found in cellulose, lignin, tannins, and chlorophyll. The C=C group of the aromatic ring is found in lignin and tannins [32, 33].

Basically, the epicarp and mesocarp of green coconut consist of cellulose, lignin and hemicelluloses, while tannins are also found [34, 35].

The tannins are considered to be chemically highly reactive, able to form intra- and intermolecular hydrogen bonds [36].

3.2. Adsorption Kinetics.
The adsorption kinetics reveal the influence of the contact time between species to be adsorbed and the adsorbent and the amount of species adsorbed [37].

For the epicarp of green coconut, the adsorption of fluoride ions reached equilibrium in 300 minutes, with final concentrations equivalent to 1.35 mg·L^{-1} (at 25°C), 1.10 mg·L^{-1} (at 35°C), and 0.90 mg·L^{-1} (at 45°C). The concentration of fluoride ions as a function of time employing epicarp as biosorbent can be seen in Figure 3.

TABLE 1: Textural properties of dried epicarp and mesocarp of green coconut.

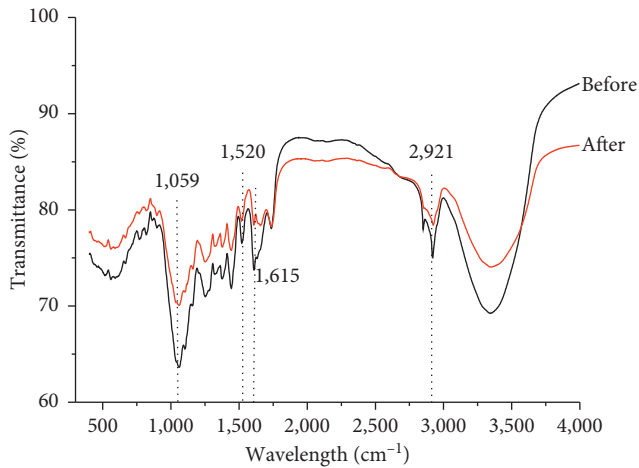|	Epicarp	Mesocarp
Specific surface area ($m^2 \cdot g^{-1}$)	3.360	5.766
Specific volume of mesopores ($cm^3 \cdot g^{-1}$)	4.08×10^{-3}	3.04×10^{-3}
Specific volume of micropores ($cm^3 \cdot g^{-1}$)	8.42×10^{-4}	1.47×10^{-3}
Mean radius of the mesopores (nm)	1.520	1.521
Mean radius of the micropores (nm)	0.226	0.152

FIGURE 1: FTIR vibrational spectra of epicarp of green coconut (before and after adsorption).
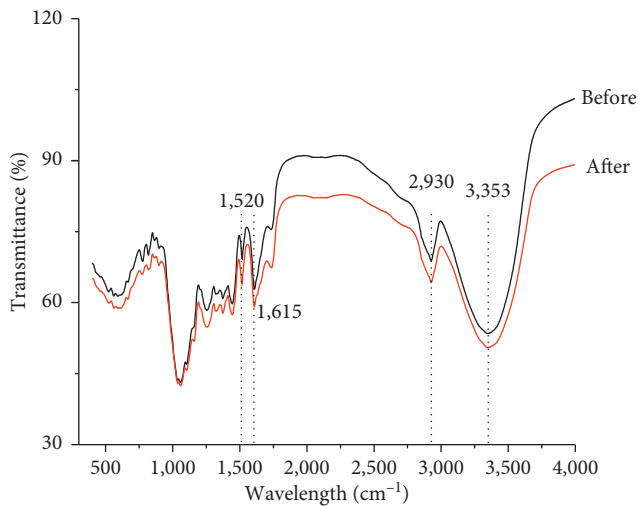

FIGURE 2: FTIR vibrational spectra of mesocarp of green coconut (before and after adsorption).
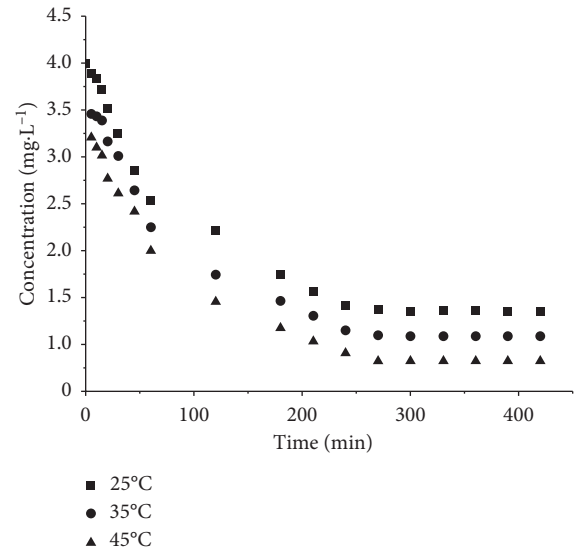

FIGURE 3: Concentration of fluoride ions as a function of time using epicarp as biosorbents.

FIGURE 4: Concentration of fluoride ions as a function of time using mesocarp as biosorbents.

For the mesocarp of green coconut, the adsorption of fluoride ions reached equilibrium in 300 minutes, with final concentrations equivalent to $0.40 \, mg \cdot L^{-1}$ (at 25°C), $0.20 \, mg \cdot L^{-1}$ (at 35°C), and $0.10 \, mg \cdot L^{-1}$ (at 45°C). Figure 4 shows the concentration of fluoride ions as a function of time using mesocarp as biosorbents.
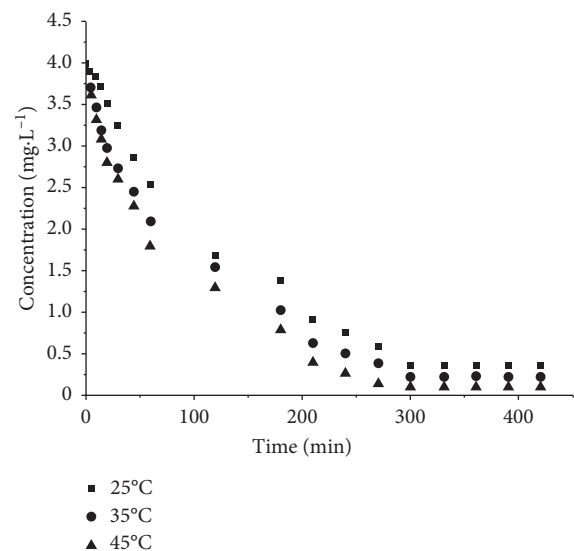
As for removal efficiency of fluoride ions, the epicarp showed 66.25% (at 25°C), 72.50% (at 35°C), and 77.50% (at 45°C). For mesocarp, removal efficiency was 90% (at 25°C), 95% (at 35°C), and 97.50% (at 45°C).

The higher removal efficiency of fluoride ions by the mesocarp may be associated with its greater specific surface area compared to the epicarp.

The kinetic parameters for adsorption of fluoride ions by epicarp and mesocarp of green coconut are summarised in Table 2.

R^2 corresponds to the coefficient of determination (dimensionless).

Table 2 shows that, using Akaike's criterion for small samples, the pseudo-first-order model is the best fit for the experimental data at 25°C, while the pseudo-second-order model is the best fit for the experimental data at 35 and 45°C.

3.3. Adsorption Isotherms. The Langmuir isotherm model suggests that adsorption occurs at homogeneous sites in the

TABLE 2: Kinetics parameters for adsorption of fluoride ions by epicarp and mesocarp of green coconut.

Model	Epicarp			Mesocarp		
Pseudo-first-order	25°C	35°C	45°C	25°C	35°C	45°C
q_e (mg·g^{-1})	0.1629	0.1742	0.1857	0.2358	0.2273	0.2323
k_1 (min^{-1})	0.0107	0.0145	0.0194	0.0072	0.0111	0.0125
R^2	0.9920	0.9850	0.9515	0.9952	0.9840	0.9821
AIC$_c$	−174.2137	−164.7537	−145.9986	−171.3698	−153.7335	−151.5198
Pseudo-second-order						
q_e (mg·g^{-1})	0.2070	0.2082	0.2120	0.3212	0.2309	0.2801
k_2 (g·mg^{-1}·min^{-1})	0.0490	0.0758	0.1120	0.0187	0.0408	0.0512
R^2	0.9876	0.9891	0.9761	0.9927	0.9927	0.9920
AIC$_c$	−166.7448	−170.2651	−158.0703	−164.2642	−167.0878	−165.1528
Elovich model						
α (mg·g^{-1}·min^{-1})	0.0054	0.0091	0.0149	0.0061	0.0092	0.0109
β (g·mg^{-1})	23.8895	24.8819	25.6593	17.1782	18.4377	18.2533
R^2	0.9733	0.9650	0.9725	0.9591	0.9767	0.9800
AIC$_c$	−153.7335	−150.3733	−155.6375	−135.0571	−147.3355	−149.5615
Intraparticle diffusion model						
k_{dif} (mg·g^{-1}·min$^{-0.5}$)	0.0092	0.0089	0.0086	0.0131	0.0121	0.0121
C_d (mg·g^{-1})	−0.0043	0.0177	0.0379	−0.0222	0.0073	0.0172
R^2	0.9396	0.9394	0.9419	0.9750	0.9697	0.9550
AIC$_c$	−139.8852	−140.0723	−142.9349	−143.4189	−142.8754	−135.8247

adsorbent, where all sites are identical and energetically equivalent and there is no interaction between the adsorbed species at the neighboring sites [38].

The Freundlich isotherm model describes equilibrium on heterogeneous surfaces and does not therefore assume a monolayer adsorption capacity. This model suggests that the amount of the species retained in the adsorbent increases as the species concentration in the solution increases [27].

The Langmuir and Freundlich constants for adsorption of fluoride ions by epicarp and mesocarp of green coconut are shown in Table 3. It can be seen that the fluoride ions adsorption isotherm data fit well with the Langmuir isotherm model, with the smallest value of Akaike's criterion for small samples.

Table 4 shows the maximum adsorption capacity of some adsorbents for the removal of fluoride ions. It can be observed that the adsorbents studied in this work present a higher maximum adsorption capacity.

3.4. Thermodynamic Analyses. The thermodynamic parameters of adsorption were calculated from the equilibrium constant k_d, determined by the graph of the Neperian logarithm of the ratio q_e/C_e as a function of q_e, extrapolating C_e to zero [43].

The thermodynamic parameters were calculated using the following equations [43]:

$$\Delta G = -R \cdot T \cdot \ln k_d,$$

$$\ln k_d = \left(\frac{\Delta S}{R}\right) - \left(\frac{\Delta H}{R}\right) \cdot \frac{1}{T}, \quad (10)$$

where ΔS is the entropy variation (kJ·mol^{-1}·K^{-1}), ΔH is the enthalpy variation (kJ·mol^{-1}), ΔG is the Gibbs free energy

variation (kJ·mol^{-1}), R is the gas constant (kJ·mol^{-1}·K^{-1}), and T is the temperature (K).

Plotting $\ln k_d$ against $1/T$ gives a straight line with slope and intercept equal to $-(\Delta H/R)$ and $(\Delta S/R)$, respectively, as shown in Figure 5.

The values of Gibbs free energy variation, entropy variation, and enthalpy variation are shown in Table 5.

Negative values for the Gibbs free energy variation indicate that the adsorptive process was spontaneous; that is, it was thermodynamically favourable. Positive values for the enthalpy variation indicate that the adsorption process was endothermic. In adsorption, endothermic processes can be associated with the energy barrier necessary for the formation of the activated adsorbent-adsorbate complex; it was necessary to provide energy to overcome the energy barrier. Positive values for the entropy variation indicate that there has been an increase in the system disorder at the solid-fluid interface during adsorption [22].

The effect of temperature on the adsorption of fluoride ions was studied by means of the Arrhenius equation in the linearised form [44]:

$$\ln k_{cin} = \ln A - \left(\frac{E_a}{R}\right) \cdot \frac{1}{T}, \quad (11)$$

where k_{cin} is the constant of the best-fit kinetic model (unit according to the model), A is the frequency factor (unit associated with the best-fit kinetic model), and E_a is the activation energy (kJ·mol^{-1}).

The parameters of the Arrhenius equation are shown in Table 6.

The activation energy is a parameter associated with the nature and intensity of the interactions between the adsorbent and the adsorbate. This energy depends on the chemical nature of the species involved and is generally employed to distinguish types of adsorption. For adsorption energy values

TABLE 3: The Langmuir and Freundlich models constants.

Model	Epicarp			Mesocarp		
Langmuir model	25°C	35°C	45°C	25°C	35°C	45°C
q_{max} (mg·g^{-1})	1.6909	2.2265	1.8176	1.8021	1.7802	3.2253
k_L (L·mg^{-1})	1.1338	1.0448	1.8537	2.0968	1.1465	1.1874
R^2	0.9689	0.9904	0.9648	0.9652	0.9594	0.9863
AIC$_c$	−43.0679	−49.5204	−37.8549	−37.5464	−35.8396	−42.9539
Freundlich model						
k_F (mg$^{(n-1/n)}$·L$^{(1/n)}$)	0.1439	0.1978	0.6290	0.5687	0.8536	1.7757
n	1.2490	1.2053	1.4515	1.3822	1.4230	1.1868
R^2	0.9595	0.9856	0.9521	0.9544	0.9468	0.9816
AIC$_c$	−41.2255	−46.6851	−35.7090	−35.6467	−33.9463	−40.8807

TABLE 4: Maximum adsorption capacity of some adsorbents for fluoride ions removal.

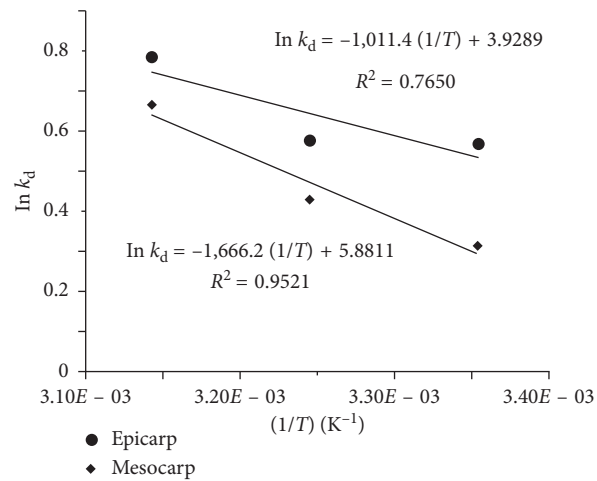| Adsorbent	q_{max} (mg·g^{-1})	Reference
Mixed rare earth oxides of activated alumina	0.7400	[39]
Modified amberlite resin	0.0610	[40]
Granular acid-treated bentonite	0.2780	[41]
Natural chitosan	1.3900	[42]
Epicarp of green coconut	2.2265 (35°C)	This work
Mesocarp of green coconut	3.2253 (45°C)	This work

FIGURE 5: The plot of $\ln k_d$ vs. $1/T$.

TABLE 5: Thermodynamic parameters for adsorption of fluoride ions on epicarp and mesocarp of green coconut.

T (°C)	Epicarp			Mesocarp		
	ΔG (kJ·mol^{-1})	ΔH (kJ·mol^{-1})	ΔS (kJ·mol^{-1}·K^{-1})	ΔG (kJ·mol^{-1})	ΔH (kJ·mol^{-1})	ΔS (kJ·mol^{-1}·K^{-1})
		8.4046	0.0327		13.8486	0.0489
25	−1.4123			−0.7802		
35	−1.4820			−1.0979		
45	−2.0766			−1.7654		

between 5 and 40 kJ·mol^{-1}, the adsorption is classified as physical, while for values between 40 and 800 kJ·mol^{-1}, it is classified as chemical [44]. It can thus be observed in Table 6 that the adsorption of the fluoride ions by the epicarp and mesocarp of green coconut is classified as chemical.

No adsorption studies on fluoride ions using the epicarp and mesocarp of green coconut could be found in the literature.

Many water sources are abandoned because of excess fluoride ions and the cost of treatment [16]. The results showed the relevant amount of fluoride ions adsorbed by the epicarp and mesocarp of green coconut in relation to other adsorbents already studied. The use of these materials as an adsorbent thus offers a promising alternative for reuse and disposal, reducing the environmental impact in industrial landfills and landfills.

TABLE 6: Parameters of the Arrhenius equation for adsorption of fluoride ions on epicarp and mesocarp of green coconut.

T (°C)	$\ln k_{cin}$	A (g·mg^{-1}·min^{-1})	E_a (kJ·mol^{-1})	R^2
Epicarp				
		3.1106×10^{14}	93.3827	0.8828
25	−4.5413			
35	−2.5797			
45	−2.1893			
Mesocarp				
		4.1560×10^{11}	77.9670	0.8492
25	−4.9337			
35	−3.1991			
45	−2.9720			

4. Conclusions

Removal of fluoride ions by the epicarp and mesocarp of green coconut was investigated. The epicarp showed removal efficiency ranging from 66.25% (at 25°C) to 77.50% (at 45°C), while the mesocarp showed removal efficiency ranging from 90% (at 25°C) to 97.50% (at 45°C).

The maximum adsorption capacity ranged from 1.6909 to 2.2265 mg·g^{-1} for the epicarp and from 1.7802 to 3.2253 mg·g^{-1} for the mesocarp. Compared with other adsorbents of fluoride ions found in the literature, these materials had high values of maximum adsorption capacity. For the two biosorbents, the pseudo-first-order kinetic model appears relevant to describe the fluoride ions adsorption at 25°C, while the pseudo-second-order kinetic model was the best fit for the experimental data at 35 and 45°C.

The thermodynamic parameters show that the adsorption of fluoride ions was a spontaneous and endothermic process for both biosorbents, and the adsorption was classified as chemical.

The adsorption data of fluoride ions fit well with the Langmuir isotherm model, suggesting that adsorption occurs at homogeneous sites in the developed biosorbents.

Data Availability

The data used to support the findings of this study are available from the corresponding author upon request.

Conflicts of Interest

The authors certify that they have no affiliations with or involvement in any organisation or entity with any financial interest.

Acknowledgments

References

[1] G. Chae, S. Yun, B. Mayer et al., "Fluorine geochemistry in bedrock groundwater of South Korea," *Science of the Total Environment*, vol. 385, no. 1–3, pp. 272–283, 2007.

[2] G. Viswanarhan, A. Jaswanth, S. Gopalakrishnan, S. S. Ilango, and G. Aditya, "Determining the optimal fluoride concentration in drinking water for fluoride endemic regions in South India," *Science of the Total Environment*, vol. 407, no. 20, pp. 5298–5307, 2009.

[3] O. Barbier, L. Arreola-Mendoza, and L. M. Del Razo, "Molecular mechanisms of fluoride toxicity," *Chemico-Biological Interactions*, vol. 188, no. 2, pp. 319–333, 2010.

[4] C. K. Diawara, S. N. Diop, M. A. Diallo, M. Farcy, and A. Deratani, "Performance of nanofiltration (NF) and low pressure reverse osmosis (LPRO) membranes in the removal of fluorine and salinity from brackish drinking water," *Journal of Water Resource and Protection*, vol. 03, no. 12, pp. 912–917, 2011.

[5] M. E. Espósito, J. D. Paoloni, M. E. Sequeira, N. M. Amiotti, and M. D. C. Blanco, "Natural contaminants in drinking waters (arsenic, boron, fluorine and vanadium) in the Southern Pampean Plain, Argentina," *Journal of Environmental Protection*, vol. 02, no. 01, pp. 97–108, 2011.

[6] P. Gwala, S. Andey, P. Nagarnaik et al., "Design and development of sustainable remediation process for mitigation of fluoride contamination in ground water and field application for domestic use," *Science of the Total Environment*, vol. 488-489, pp. 588–594, 2014.

[7] C. Murutu, M. S. Onyango, A. Ochieng, and F. A. O. Otieno, "Fluoride removal performance of phosphoric acid treated lime: breakthrough analysis and point-of-use system performance," *Water SA*, vol. 38, no. 2, pp. 279–286, 2012.

[8] N. J. Chinoy and M. V. Narayana, "In vitro fluoride toxicity in human spermatozoa," *Reproductive Toxicology*, vol. 8, no. 2, pp. 155–159, 1994.

[9] D. Shanthakumari, S. Srinivasalu, and S. Subramanian, "Effect of fluoride intoxication on lipidperoxidation and antioxidant status in experimental rats," *Toxicology*, vol. 204, no. 2-3, pp. 219–228, 2004.

[10] S. J. S. Flora, M. Mittal, and D. Mishra, "Co-exposure to arsenic and fluoride on oxidative stress, glutathione linked enzymes, biogenic amines and DNA damage in mouse brain," *Journal of the Neurological Sciences*, vol. 285, no. 1-2, pp. 198–205, 2009.

[11] R. Srikanth, K. S. Viswanatham, F. Kahsai, A. Fisahatsion, and M. Asmellash, "Fluoride in groundwater in selected villages in Eritrea (North East Africa)," *Environmental Monitoring and Assessment*, vol. 75, no. 2, pp. 169–177, 2002.

[12] L. Fewtrell, S. Smith, D. Kay, and J. Bartram, "An attempt to estimate the global burden of disease due to fluoride in drinking water," *Journal of Water and Health*, vol. 4, no. 4, pp. 533–542, 2006.

[13] M. A. Dar, K. Sankar, and I. A. Dar, "Fluorine contamination in groundwater: a major challenge," *Environmental Monitoring and Assessment*, vol. 173, no. 1–4, pp. 955–968, 2011.

[14] J. O. Odiyo and R. Makungo, "Fluoride concentrations in groundwater and impact on human health in Siloam Village, Limpopo province, South Africa," *Water SA*, vol. 38, no. 5, pp. 731–736, 2012.

[15] M. C. T. Cangussu, P. C. Narvai, R. Castellanos Fernandez, and V. A. Djehizian, "A fluorose dentária no Brasil: uma revisão crítica," *Cadernos de Saúde Pública*, vol. 18, no. 1, pp. 7–15, 2002.

[16] M. Habuda-Stanić, M. E. Ravančić, and A. Flanagan, "A review on adsorption of fluoride from aqueous solution," *Materials*, vol. 7, no. 9, pp. 6317–6366, 2014.

[17] O. A. Carrijo, R. S. d. Liz, and N. Makishima, "Fibra da casca do coco verde como substrato agrícola," *Horticultura Brasileira*, vol. 20, no. 4, pp. 533–535, 2002.

[18] D. V. Bitencourt and A. Pedrotti, "Usos da casca de coco: estudo das viabilidades de implantação de usina de beneficiamento de fibra de coco em Sergipe," *Revista da Fapese*, vol. 4, no. 2, pp. 113–122, 2008.

[19] A. P. Martins, R. A. Sanches, P. L. R. Silva, C. Borelli, T. Watanabe, and J. P. P. Marcicano, "O problema do pós-consumo do coco no Brasil: alternativas e sustentabilidade," *Sustentabilidade em Debate*, vol. 7, no. 1, pp. 44–57, 2016.

[20] A. C. A. Lima, R. F. Nascimento, F. F. Sousa, J. M. Filho, and A. C. Oliveira, "Modified coconut shell fibers: a green and economical sorbent for the removal of anions from aqueous solutions," *Chemical Engineering Journal*, vol. 185-186, pp. 274–284, 2012.

[21] L. S. Clesceri, A. E. Greenberg, and A. D. Eaton, *Standard Methods for the Examination of Water and Wastewater*, American Public Health Association, Washington, DC, USA, 20 edition, 1999.

[22] M. Suzuki, *Adsorption Engineering*, Elsevier Science Publishers, Amsterdam, Netherlands, 1990.

[23] Y. S. Ho, J. C. Y. Ng, and G. Mckay, "Kinetics of pollutant sorption by biosorbents: review," *Separation and Purification Methods*, vol. 29, no. 2, pp. 189–232, 2000.

[24] Y. S. Ho, "Citation review of Lagergren kinetic rate equation on adsorption reactions," *Scientometrics*, vol. 59, no. 1, pp. 171–177, 2004.

[25] H. Qiu, L. Lv, B.-c. Pan, Q.-j. Zhang, W.-m. Zhang, and Q.-x. Zhang, "Critical review in adsorption kinetic models," *Journal of Zhejiang University-Science A*, vol. 10, no. 5, pp. 716–724, 2009.

[26] S. Adachi, C. Panintrarux, and R. Matsuno, "Methods for estimating the parameters of nonlinear adsorption isotherms of Langmuir and Freundlich types from a response curve of pulse input of an adsorbate," *Bioscience, Biotechnology, and Biochemistry*, vol. 61, no. 10, pp. 1626–1633, 1997.

[27] C. Ng, J. N. Losso, W. E. Marshall, and R. M. Rao, "Freundlich adsorption isotherms of agricultural by-product-based powdered activated carbons in a geosmin-water system," *Bioresource Technology*, vol. 85, no. 2, pp. 131–135, 2002.

[28] C. M. Hurvich and C.-L. Tsai, "Regression and time series model selection in small samples," *Biometrika*, vol. 76, no. 2, pp. 297–307, 1989.

[29] L. Mayor and A. M. Sereno, "Modelling shrinkage during convective drying of food materials: a review," *Journal of Food Engineering*, vol. 61, no. 3, pp. 373–386, 2004.

[30] W. L. Mccabe, J. C. Smith, and P. Harriot, *Unit Operations of Chemical Engineering*, McGraw-Hill Book Co, Singapore, 5 edition, 1993.

[31] D. L. Pavia, G. M. Lampman, G. S. Kriz, and J. R. Vyvyan, *Introdução à Espectroscopia*, Cengage Learning, São Paulo, Brazil, 2012.

[32] D. Fengel and G. Wegener, *Wood: Chemistry, Ultrastructure and Reactions*, Walter de Gruyter & Co., Berlin, Germany, 1989.

[33] N. M. Streit, L. P. Canterle, M. W. d. Canto, and L. H. H. Hecktheuer, "As clorofilas," *Ciência Rural*, vol. 35, no. 3, pp. 748–755, 2005.

[34] A. I. S. Brígida and M. F. Rosa, "Determinação do teor de taninos na casca de coco verde (*Cocos nucifera*)," in *Proceedings of the Interamerican Society for Tropical Horticulture*, vol. 47, pp. 25–27, Fortaleza, Brazil, August-September 2003.

[35] A. C. Benassi, C. J. Fanton, and E. N. Santana, *O Cultivo do Coqueiro- anão-verde: Tecnologias de produção*, Incaper, Vitória, Brazil, 2013.

[36] J. M. Monteiro, U. P. d. Albuquerque, E. d. L. Araújo, and E. L. C. Amorim, "Taninos: uma abordagem da química à ecologia," *Química Nova*, vol. 28, no. 5, pp. 892–896, 2005.

[37] A. Dabrowski, "Adsorption—from theory to practice," *Advances in Colloid and Interface Science*, vol. 93, no. 1–3, pp. 135–224, 2001.

[38] I. Langmuir, "The constitution and fundamental properties of solids and liquids. Part I. Solids," *Journal of the American Chemical Society*, vol. 38, no. 11, pp. 2221–2295, 1916.

[39] S. Ghori and K. K. Pant, "Investigation on the column performance of fluoride adsorption by activated alumina in a fixed bed," *Chemical Engineering Journal*, vol. 98, no. 1-2, pp. 165–173, 2004.

[40] I. B. Solangi, S. Memon, and M. I. Bhanger, "An excellent fluoride sorption behavior of modified amberlite resin," *Journal of Hazardous Materials*, vol. 176, no. 1-3, pp. 186–192, 2010.

[41] Y. Ma, F. Shi, X. Zheng, J. Ma, and C. Gao, "Removal of fluoride from aqueous solution using granular acid-treated bentonite (GHB): batch and column studies," *Journal of Hazardous Materials*, vol. 185, no. 2-3, pp. 1073–1080, 2011.

[42] P. Miretzky and A. F. Cirelli, "Fluoride removal from water by chitosan derivatives and composites: a review," *Journal of Fluorine Chemistry*, vol. 132, no. 4, pp. 231–240, 2011.

[43] J. W. Biggar and M. W. Cheung, "Adsorption of picloram (4-amino-3,5,6-trichloropicolinic acid) on panoche, ephrata, and palouse soils: a thermodynamic approach to the adsorption mechanism," *Soil Science Society of America Journal*, vol. 37, no. 6, pp. 863–868, 1973.

[44] D. M. Ruthven, *Principles of Adsorption and Adsorption Process*, John Wiley & Sons, New York, NY, USA, 1984.